



Structural, Optical and Dielectric Properties of (PS- In_2O_3 / $\text{ZnCoFe}_2\text{O}_4$) Nanocomposites



Noor Hayder, Majeed Ali Habeeb and Ahmed Hashim*

University of Babylon, College of Education for Pure Sciences, Department of Physics, Iraq.

The (PS- In_2O_3 / $\text{ZnCoFe}_2\text{O}_4$) nanocomposites have been prepared by using solution casting method. The structural, optical and dielectric properties of (PS- In_2O_3 / $\text{ZnCoFe}_2\text{O}_4$) nanocomposites have been studied to use it for different optoelectronics applications. The structural properties include FTIR, optical microscope and SEM. The results of optical properties for (PS- In_2O_3 / $\text{ZnCoFe}_2\text{O}_4$) nanocomposites showed that the absorbance, absorption coefficient, refractive index, extinction coefficient, dielectric constants and optical conductivity of (PS- In_2O_3) nanocomposites were increased with the increase in $\text{ZnCoFe}_2\text{O}_4$ nanoparticles concentrations while the transmittance and energy band gap were decreased with the increase of the $\text{ZnCoFe}_2\text{O}_4$ nanoparticles concentrations. The (PS- In_2O_3 / $\text{ZnCoFe}_2\text{O}_4$) nanocomposites have high absorbance in the UV-region. The results of dielectric properties showed that the dielectric constant, dielectric loss and A.C electrical conductivity of (PS- In_2O_3) nanocomposites increase with increase in $\text{ZnCoFe}_2\text{O}_4$ nanoparticles concentrations. The dielectric constant and dielectric loss decrease while the electrical conductivity increases with an increase in frequency.

Keywords: Polystyrene, Nanocomposites, Optical properties, Dielectric, $\text{ZnCoFe}_2\text{O}_4$.

Introduction

Nanotechnology has attracted a great deal of attention in the last few years as miniaturization and nanomaterials are often foreseen to be the key for a sustainable future. In this regard, an essential part of the scientific community is currently focused on a very challenging and relevant research's direction, which is the synthesis of novel nanostructured hybrid materials capable of absorbing the photonic energy coming from the sunlight with the aim of turning it into electrical or chemical energy. Whereas, growing concerns regarding energy and environmental problems have stimulated extensive researches on solar energy utilizations. Among them, various strategies are explored for photocatalytic hydrogen production for fuel cells and/or degradation of organic dyes using semiconductor photocatalysts. From the point of view of the materials, photocatalysts require a series of characteristic properties depending on their applications, including particle size, specific

surface area or space between the electronic levels, among others [1]. The applications of nanocomposites are quite promising in the fields of microelectronic packaging, optical integrated circuits, automobiles, drug delivery, sensors, injection molded products, membranes, packaging materials, aerospace, coatings, adhesives, fire-retardants, medical devices, consumer goods, etc[2]. By mixing organic molecules and inorganics at the nano level, robust materials, called organic-inorganic hybrids, are created, which have multiple functions originating from both components [3]. Because of their high durability, hybrids are regarded as a platform for realizing advanced optoelectronic materials containing conjugated molecules and polymers [4]. By mixing organic molecules and inorganics at the nano level, robust materials, called organic-inorganic hybrids, are created, which have multiple functions originating from both components. Because of their high durability, hybrids are regarded as a platform for realizing advanced optoelectronic materials

*Corresponding author e-mail: ahmed_taaay@yahoo.com

Received 10/07/2019; Accepted 2/10/2019

DOI: 10.21608/ejchem.2019.14646.1887

©2019 National Information and Documentation Center (NIDOC)

containing conjugated molecules and polymers. For example, electric-conductive hybrids are obtained by introducing conductive organic crystals into a polymer hybrid matrix based on silica. In particular, the resulting hybrids show a waterproof character and higher heat resistance than that of the pristine organic crystal. By loading a series of conjugated molecules onto hybrid matrices, multiple optical properties are readily expressed. Intense white-light luminescence is observed from dye-loaded robust hybrids. Thus, hybrid formation is currently recognized as a valid strategy for enhancing durability of organic products including conjugated polymers. However, hybrid formation is usually performed via the sol-gel reaction in polar solvents with acid or base catalysts. Thereby, aggregation followed by generation of inhomogeneity and degradation of conjugated polymers is often induced during the sol-gel reactions. Furthermore, carrier-transport ability could decrease after hybrid formation compared to that of the pristine organic material due to intrinsic high electric resistance of silicate. Thus, our next challenge is not only to establish the facile manner for hybrid formation without critical losses of electric properties of conjugated polymers but also to systematically study the electric properties of the polymers inside hybrids [5]. Nanocomposite materials have been extensively used in electrical applications. The fact that they are often made up of at least two constituents or phases enables us to tailor materials for special purposes. The electrical properties of a composite system are determined by the properties of the constituents, interaction between them, and geometrical configuration. In designing composite materials with specified properties for electrical applications, one should take these parameters into consideration [6]. Polystyrene (PS) is an amorphous polymer with bulky side groups. General purposes PS are hard, rigid, and transparent at room temperature and glass like thermoplastic material which can be softened and distorted under heat. It is soluble in aromatic hydrocarbon solvents, cyclohexane and chlorinated hydrocarbons [7]. In this paper, preparation of (PS-In₂O₃/ZnCoFe₂O₄) nanocomposites and studying their structural, optical and dielectric properties.

Materials and Methods

The materials used in this paper are polystyrene (PS), indium oxide nanoparticles (In₂O₃ NPs), zinc cobalt oxides (ZnCoFe₂O₄). The (PS-In₂O₃) nanocomposites were prepared by concentration 98:2. The ZnCoFe₂O₄ nanoparticles

were added to (PS-In₂O₃) nanocomposites with weight percentages are (0,2,4,6 and 8) wt.%. The specimens were prepared using casting technique with thickness ranged between (108-120) μm. The spectrophotometer's double beam (Shimadzu, UV-18000 A) was used to measure the optical properties of (PS-In₂O₃-ZnCoFe₂O₄) nanocomposites in wavelength (200–800) nm. The dielectric properties (dielectric constant, dielectric loss, A.C electrical conductivity) of (PS-In₂O₃/ZnCoFe₂O₄) nanocomposites were measured by using (LC Meter) in the frequency (f) range (100 Hz -5 MHz) at room temperature.

Absorption coefficient (α) is defined by following equation [8]:

$$\alpha = 2.303A/t \quad \dots \dots \dots (1)$$

Where A: is the absorbance and t: is the sample thickness.

The indirect transition model for amorphous semiconductors is [9]:

$$\alpha h\nu = B(h\nu - E_g^{opt})^r \quad (2)$$

Where B is a constant, $h\nu$ is the photon energy, E_g is the optical energy band gap,

$r = 2$ for allowed indirect transition and

$r = 3$ for forbidden indirect transition.

The Refractive index (n) is given by following equation [9]:

$$n = (1+R^{1/2}) / (1-R^{1/2}) \quad \dots \dots \dots (3)$$

Where R is the reflectance.

The extinction coefficient (k) is calculated by using the following equation [9]:

$$K = \alpha \lambda / 4\pi \quad \dots \dots \dots (4)$$

The dielectric constant is divided into two parts real (ϵ_1), and imaginary (ϵ_2). The real and imaginary parts of dielectric constant (ϵ_1 and ϵ_2) are calculated by using equations [10]:

$$\epsilon_1 = n^2 - k^2 \quad \dots \dots \dots (5)$$

$$\epsilon_2 = 2nk \quad \dots \dots \dots (6)$$

The measured capacitance, C(w) was used to calculate the dielectric constant, $\epsilon'(w)$ using the

following equation [11]:

$$\epsilon' = \frac{C_P}{C_O} \quad \dots\dots(7)$$

$$\epsilon'' = \epsilon'D \quad \dots\dots(8)$$

The dissipated power in the insulator is represented by the existence of alternating potential as a function of the alternating conductivity, using:

$$\sigma_{A.C} = W\epsilon''\epsilon_o \quad (9)$$

\dot{O}_{AC} is a measurement for the generated temperature in the insulating material resulting from the rotation of the dipoles in their positions, (or the vibration of the charges) as a result of the alternating of the field [11].

Results and Discussion

Figure 1 shows the images of (PS-In₂O₃/ZnCoFe₂O₄) nanocomposites for samples with different concentrations of In₂O₃ nanocomposites and different concentrations of Ferrite ZnCoFe₂O₄ at magnification power (40X). The figure shows that the ZnCoFe₂O₄ nanoparticles are aggregated as clusters at lower concentrations. When increasing the concentrations of ZnCoFe₂O₄ nanoparticles, the nanoparticles form paths of network inside the (PS). Figure 2 shows the SEM images (PS-In₂O₃/ZnCoFe₂O₄) nanocomposites. Scanning electron microscopy has been used to study the compatibility between various components of the polymers, In₂O₃ and ZnCoFe₂O₄ nanoparticles. The films exhibit uniform density of grain distribution at surface morphology and surfaces morphology of the (PS-In₂O₃/ZnCoFe₂O₄) nanocomposites show many aggregates or chunks randomly distributed of nanoparticles on the films surface. The results show an increase in the number of aggregations on the surface in accordance with increasing [12]. Figure 3 shows the FTIR spectra of pure polystyrene take at room temperature in the range 4000–500 cm⁻¹. The polystyrene doped by In₂O₃ and ZnCoFe₂O₄ nanoparticles. The characteristic peaks around 3260 cm⁻¹ in the spectra are due to the presence of the stretching vibration of hydroxyl group OH of polystyrene, while the spectral bands between 3500 and 3900 cm⁻¹ are due to OH stretching vibration of polystyrene, respectively and the bands around 2921 cm⁻¹ correspond to the CH₂ asymmetric stretching. The C=O band at about

1705 cm⁻¹ is important for further discussions, the position of this band indicates that the carboxylic acid groups form dimers. The sharp band 1085 cm⁻¹ corresponds to C-O stretching of acetyl groups present on the polystyrene backbone that remains the same for undoped but broadens for doped samples and the peak observed at about 650 cm⁻¹ is due to the OH out of plane. The figure indicates the bonding nature between In₂O₃/ZnCoFe₂O₄ nanoparticles and polystyrene [13].

Figure 4 shows the variation of the optical absorbance spectra of (PS-In₂O₃/ZnCoFe₂O₄) nanocomposites with the photon wavelength for different concentrations of ZnCoFe₂O₄ nanoparticles. Figure 5 shows that transmittance spectrum as a function of wavelength for (PS-In₂O₃/ZnCoFe₂O₄) nanocomposite. From the figures that absorbance increases and transmittance decreases with the increase in the concentration of ZnCoFe₂O₄ nanoparticles which is related to the increase in the number of charge carriers [14-21]. The absorption coefficient of nanocomposites is shown in Fig. 6. The figure shows that the absorption coefficient of (PS-In₂O₃/ZnCoFe₂O₄) nanocomposites increases with increase of ZnCoFe₂O₄ nanoparticles concentrations, this increase attributed to increase the number of charge carriers which causes to increase the absorbance. Figures 7 and 8 show the energy band gap of nanocomposites. From the values of the absorption coefficient, it can be concluded that the nanocomposites have indirect energy band gap, it decreases with increasing the ZnCoFe₂O₄ nanoparticles, this behavior is due to the creation of levels in the energy gap [22-25].

Figure 9 shows the variation of refractive index (n) with photon energy. The values of refractive index increase exponentially with increasing photon energy. This increase indicates that the electromagnetic radiation passing through the material is faster in the low photon energy. Figure 10 represents the variation of the extinction coefficient (k) with the incident photon energy. In this figure the variation is simple in the low energy region while the variation increased in the high photon energy region this behavior may be as a result to the variation of the absorption coefficient which leads to spectral deviation in the location of the charge polarization at the attenuation coefficient due to the losses in the energy of the electron transition between the energy bands [26].

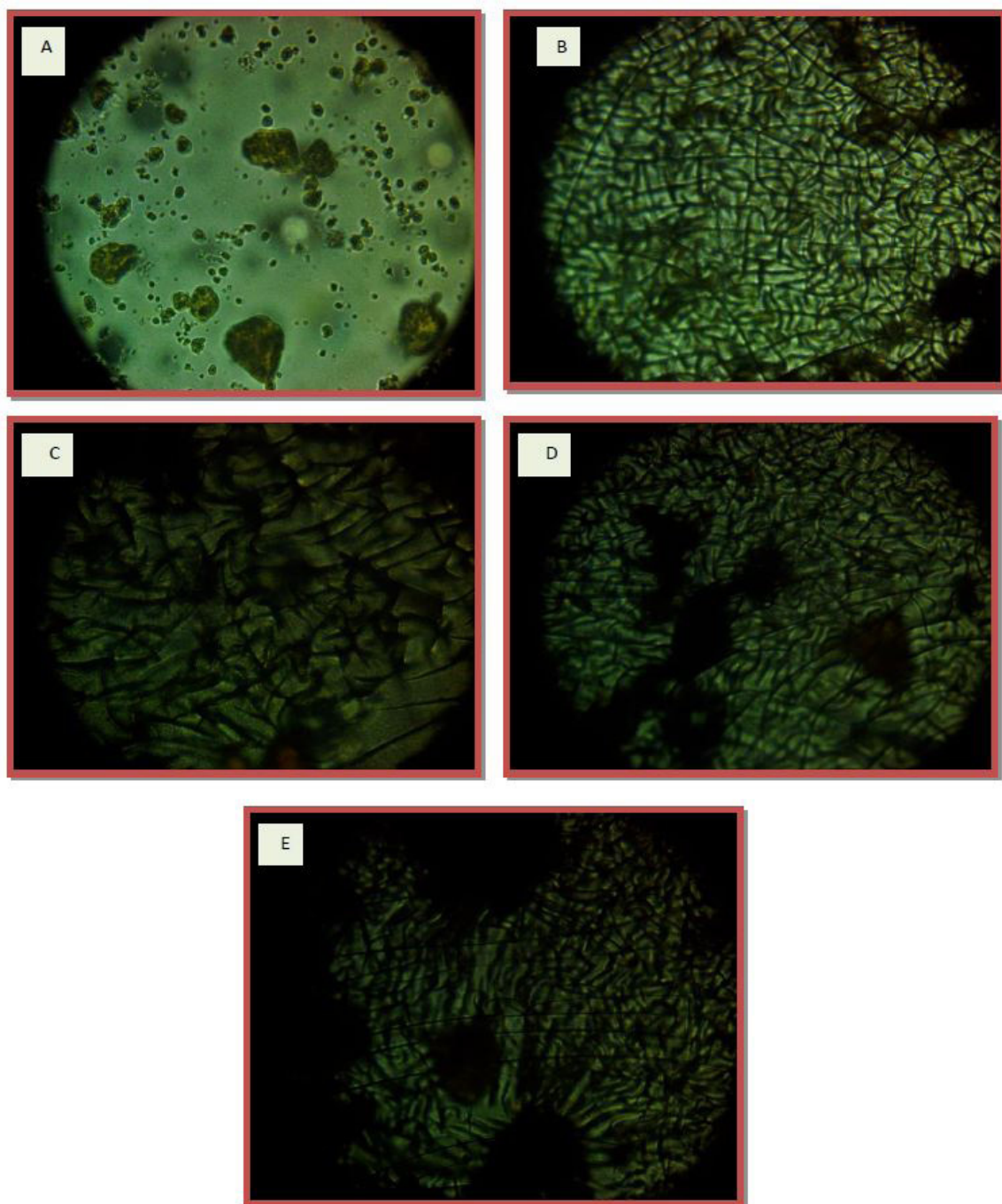


Fig. 1. Photomicrographs (40X) for (PS- In_2O_3 / $\text{ZnCoFe}_2\text{O}_4$) nanocomposites (A) for (PS- In_2O_3) (B) for 2wt.% $\text{ZnCoFe}_2\text{O}_4$ nanoparticles, (C) for 4wt.% $\text{ZnCoFe}_2\text{O}_4$ nanoparticles, (D) for 6wt.% $\text{ZnCoFe}_2\text{O}_4$ nanoparticles, (E) for 8wt.% $\text{ZnCoFe}_2\text{O}_4$ nanoparticles.

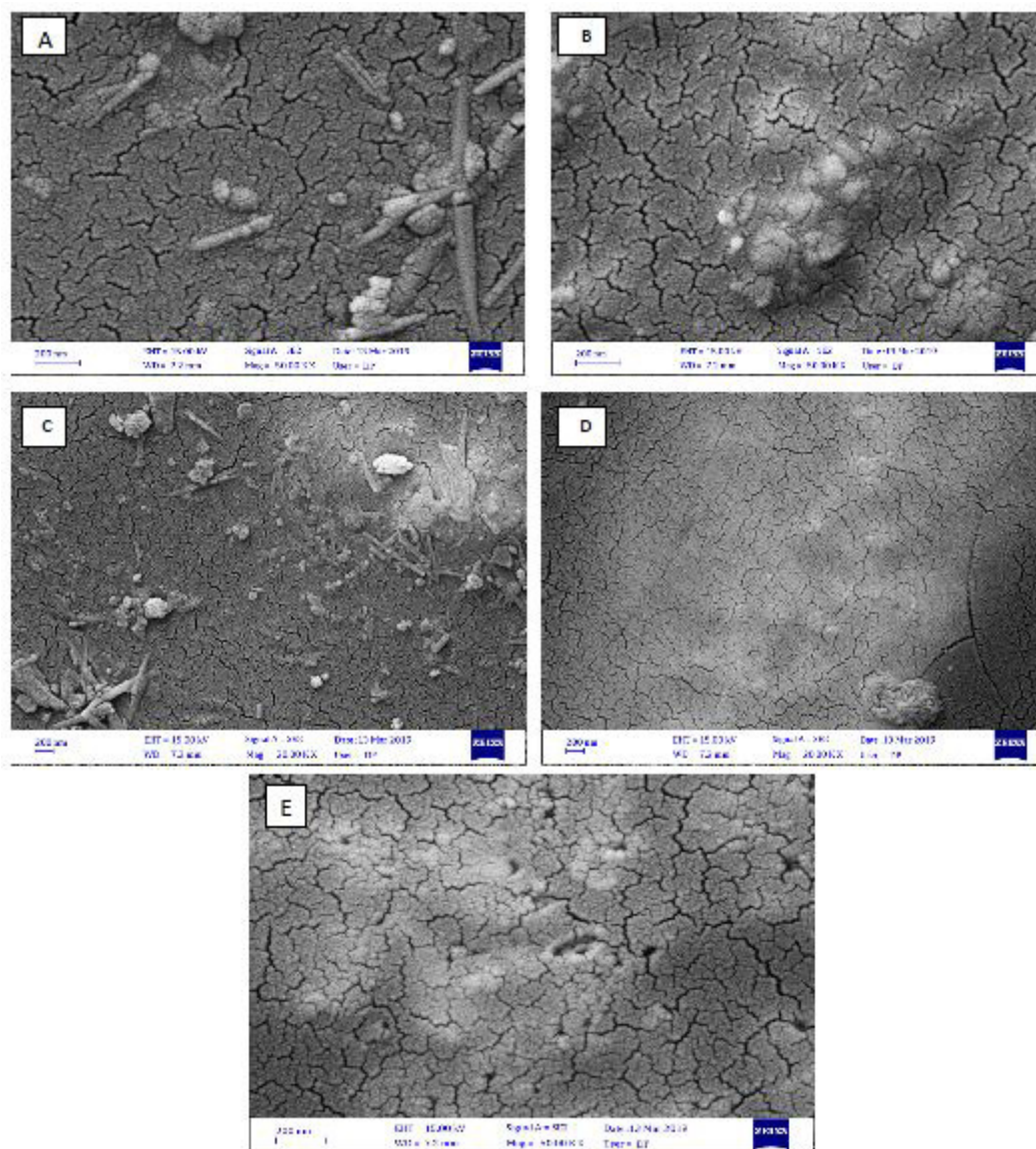


Fig. 2. SEM images of (PS- $\text{In}_2\text{O}_3/\text{ZnCoFe}_2\text{O}_4$) nanocomposites, (A) for (PS- In_2O_3), (B) 2 wt.% $\text{ZnCoFe}_2\text{O}_4$ nanoparticles, (C) 4 wt.% $\text{ZnCoFe}_2\text{O}_4$ nanoparticles, (D) 6 wt.% $\text{ZnCoFe}_2\text{O}_4$ nanoparticles, (E) 8 wt.% $\text{ZnCoFe}_2\text{O}_4$ nanoparticles.

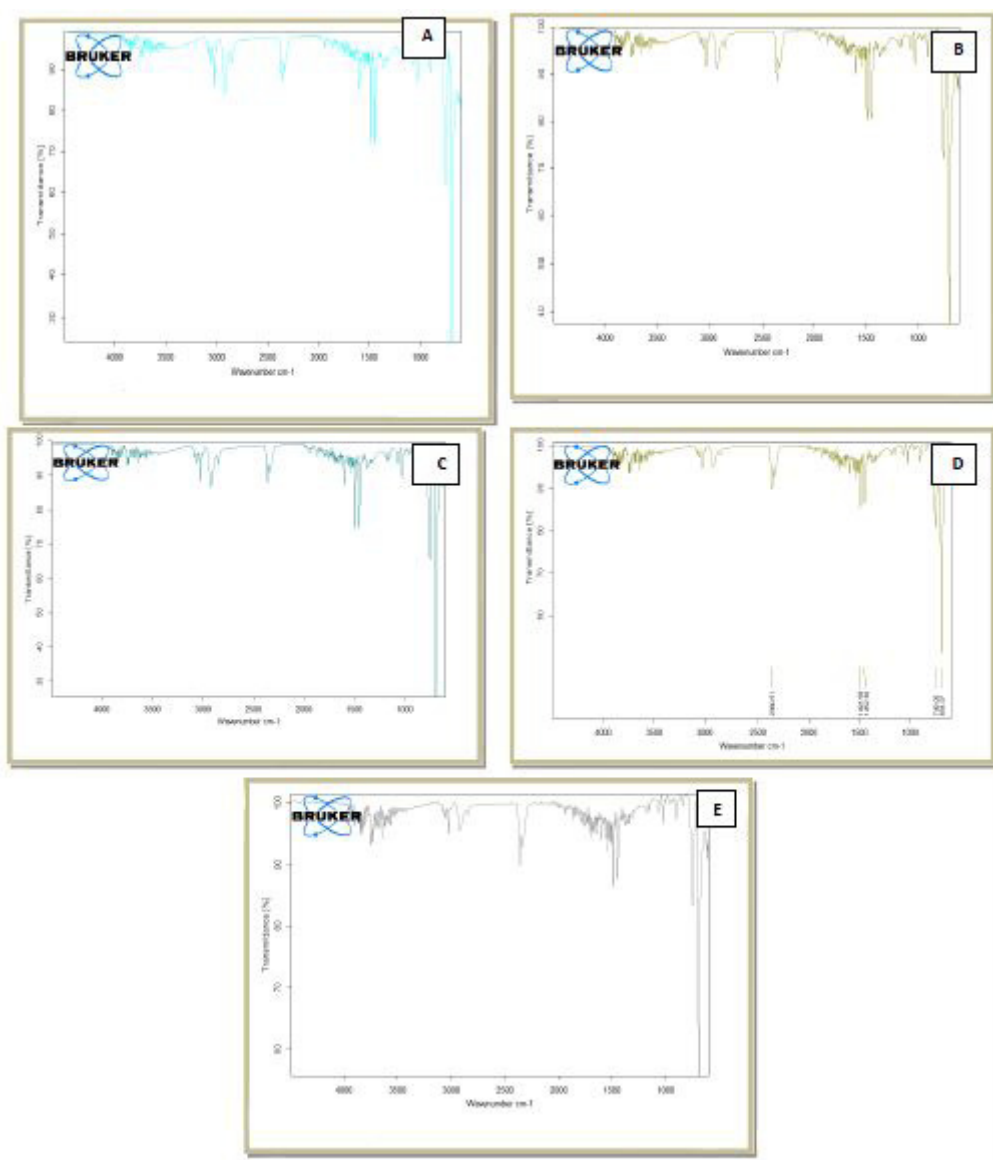


Fig. 3. FTIR spectra for (PS- $\text{In}_2\text{O}_3/\text{ZnCoFe}_2\text{O}_4$) nanocomposites: (A) for (PS- In_2O_3), (B) 2 wt.% $\text{ZnCoFe}_2\text{O}_4$, (C) 4 wt.% $\text{ZnCoFe}_2\text{O}_4$, (D) 6 wt.% $\text{ZnCoFe}_2\text{O}_4$, (E) 8 wt.% $\text{ZnCoFe}_2\text{O}_4$

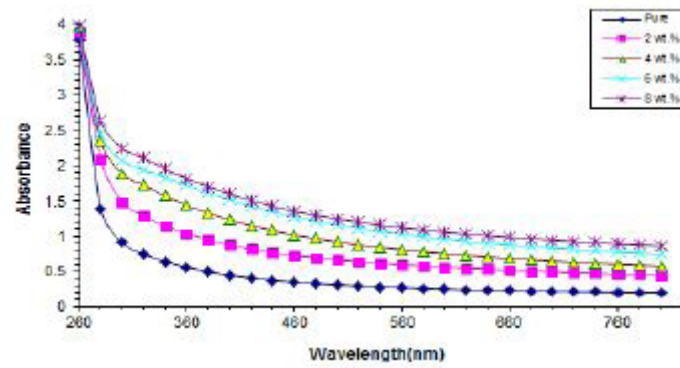


Fig. 4. Variation of absorbance for (PS- $\text{In}_2\text{O}_3/\text{ZnCoFe}_2\text{O}_4$) nanocomposites with wavelength.

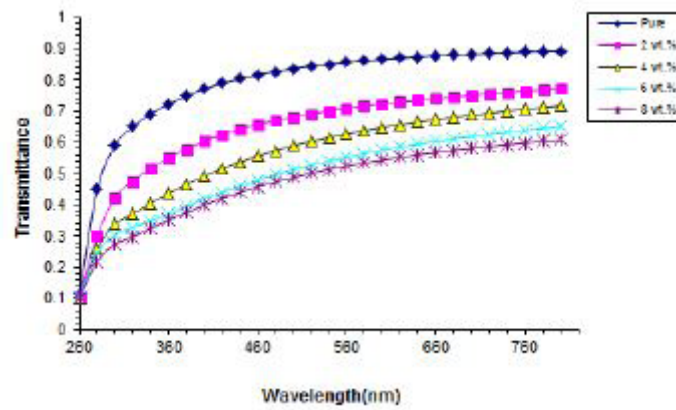


Fig. 5. Variation of transmittance for (PS- $\text{In}_2\text{O}_3/\text{ZnCoFe}_2\text{O}_4$) nanocomposites with wavelength.

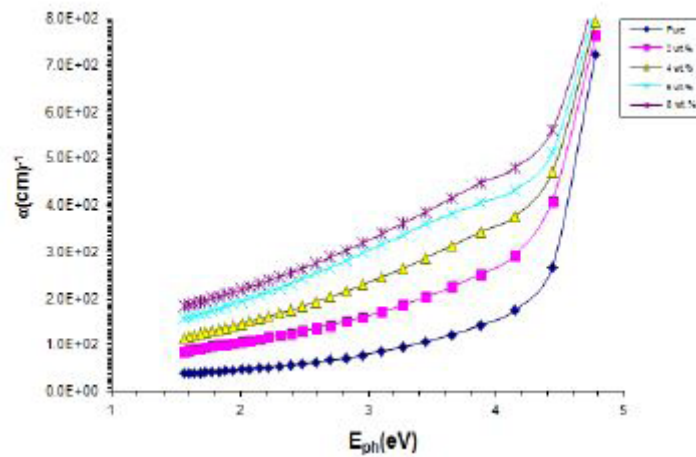


Fig. 6. Variation of absorption coefficient (α) for (PS- $\text{In}_2\text{O}_3/\text{ZnCoFe}_2\text{O}_4$) nanocomposites with photon energy.

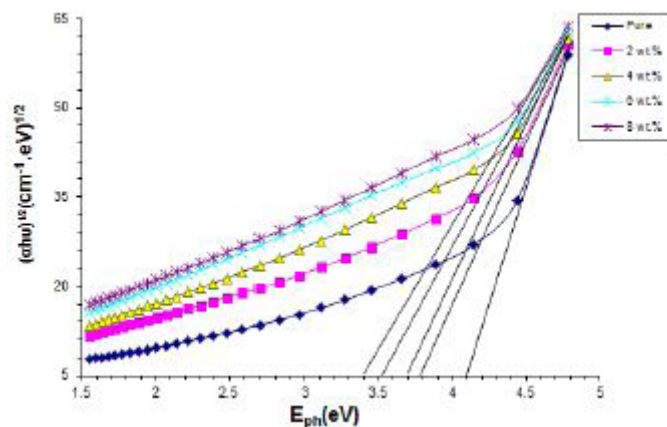


Fig. 7. Variation of $(\alpha h\nu)^{1/2}$ for (PS-In₂O₃/ZnCoFe₂O₄) nanocomposites with photon energy.

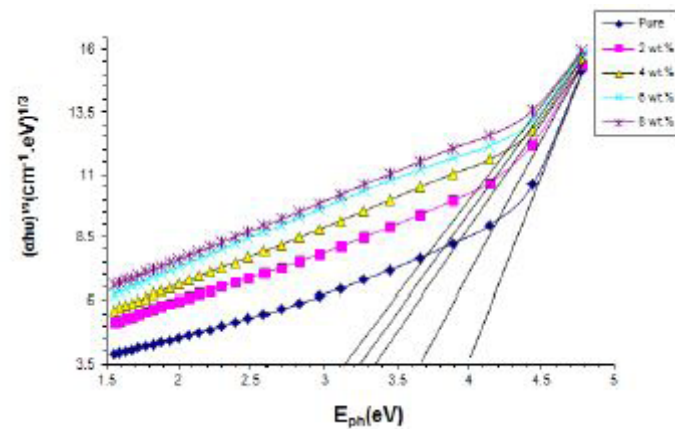


Fig. 8. Variation of $(\alpha h\nu)^{1/3}$ for (PS-In₂O₃/ZnCoFe₂O₄) nanocomposites with photon energy.

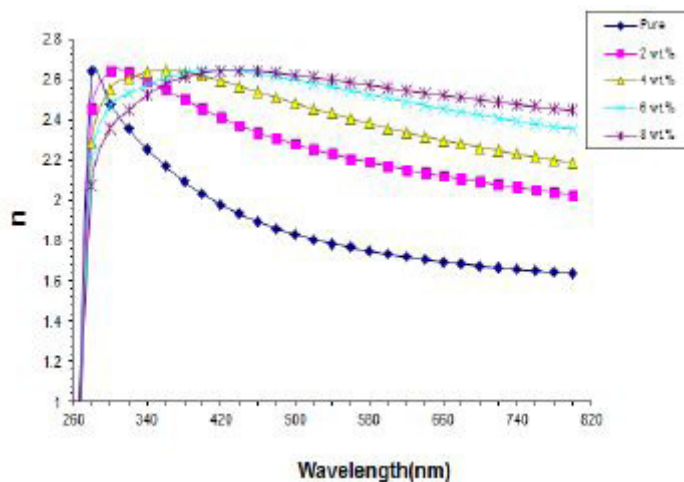


Fig. 9. Variation of refractive index for (PS-In₂O₃/ZnCoFe₂O₄) nanocomposites with wavelength.

Figure 11 shows the real dielectric constant of (PS-In₂O₃/ZnCoFe₂O₄) nanocomposites as a function of the photon energy, while Figure 12 displays the imaginary dielectric constant as a function of the photon energy. Figures 11 and 12 show that the real and imaginary parts of the dielectric constant decrease with an increase in the photon energy. The data on the real and imaginary parts of the dielectric constant provide knowledge concerning the loss factor, which is the ratio between the imaginary and real parts of the dielectric constant. These results indicate that, in the synthesized material, the loss factor increases with a decrease in the photon energy. The real part of the dielectric constant decreases a little-bit rapidly with an increase in the photon energy in the higher energy region but it decreases gradually in the lower one. However, the imaginary part of the dielectric constant decreases gradually with an increase in the photon energy [26]. The optical conductivity is one of the powerful tools for studying the electronic states in materials. The plot of the optical conductivity of (PS-In₂O₃/ZnCoFe₂O₄) nanocomposites versus the photon energy is depicted in Fig. 13. The spectrum indicates that the optical conductivity increases with the photon energy which is due to a decrease in the direct band gap due to the addition of the dopant, the optical conductivity increases. It is very clear from the graph that the optical conductivity increases with the doping of material [27].

Figure 14 shows the variation of dielectric constant with concentrations of nanoparticles for (PS-In₂O₃/ZnCoFe₂O₄) nanocomposites, at 100Hz. The dielectric constant of nanocomposites is calculated by using Equation (7). As shown in the figure, the dielectric constant of nanocomposites increases with the increasing of the concentration of ZnCoFe₂O₄ nanoparticles. This behavior could be interpreted from interfacial polarization inside the nanocomposites in applied alternating electric field and the increasing of the charge carriers [28].

The variation of dielectric constant of nanocomposites with frequency is shown in Fig. 15. The figure shows that dielectric constant decreases with the increasing of frequency of applied field, this may be attributed to the tendencies of dipole in nanocomposites samples for orienting themselves in the directions of the applied electrical fields and decreasing of space charge polarization to the total polarization. These are similar to the results of researchers [29].

Figure 16 shows the variation of the A.C electrical conductivity of (PS-In₂O₃/ZnCoFe₂O₄) nanocomposite with frequency. The figure shows that the electrical conductivity increases when increasing the frequency this can be attributed to the interfacial polarization [30].

The variation of electrical conductivity as function of the ZnCoFe₂O₄ concentration of (PS-In₂O₃/ZnCoFe₂O₄) nanocomposites at 100Hz is shown in Fig (17). The A.C electrical conductivity increases with an increase in ZnCoFe₂O₄ nanoparticles which is due to increase of the charge carrier density in polymer matrix [31-36].

Figure 18 shows the variation of the dielectric loss of (PS-In₂O₃/ZnCoFe₂O₄) nanocomposites with frequency of applied electric field. The figure shows that the dielectric loss of nanocomposites decreases with increase of frequency of applied electric field, this behavior is attributed to a decrease of the space charge polarization contribution. In addition, the dielectric loss has high value for (PS-In₂O₃/ZnCoFe₂O₄) nanocomposites at low frequency and decreases with the increasing of the frequency [37].

The dielectric loss of (PS-In₂O₃/ZnCoFe₂O₄) nanocomposites increases with increasing of the concentration of nanoparticles, as shown in Fig. 19. This related to the increases of the charge carriers number. At low concentrations of nanoparticles, it forms clusters shape, when the concentration of nanoparticles reaches to 8 wt.%, the nanoparticles form a continuous network in the nanocomposites. The results are similar to the results of the previous researcher [38].

Conclusions

The absorbance of (polystyrene-indium oxide) increases with increase of the ZnCoFe₂O₄ nanoparticles concentrations. The (PS-In₂O₃/ZnCoFe₂O₄) have higher absorbance at UV region. The energy band gap of (PS-In₂O₃) nanocomposites decreases with increase in ZnCoFe₂O₄ nanoparticles concentrations. The absorption coefficient (α), extinction coefficient (k), refractive index (n) and real and imaginary dielectric constants are increasing with increase of the weight percentages of the ZnCoFe₂O₄ nanoparticles concentrations. The dielectric constant and dielectric loss decreases while the A.C electrical conductivity increases with increase in frequency. The dielectric constant, dielectric loss and A.C electrical conductivity are increased with increasing of the ZnCoFe₂O₄ wt.% content. From the results, the (PS-In₂O₃/ZnCoFe₂O₄) nanocomposites may be used for different optoelectronics applications.

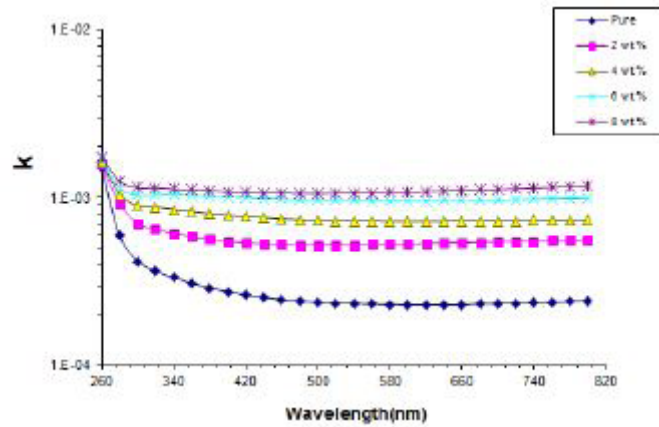


Fig. 10. Variation of extinction coefficient for (PS-In₂O₃/ ZnCoFe₂O₄) nanocomposites with wavelength.

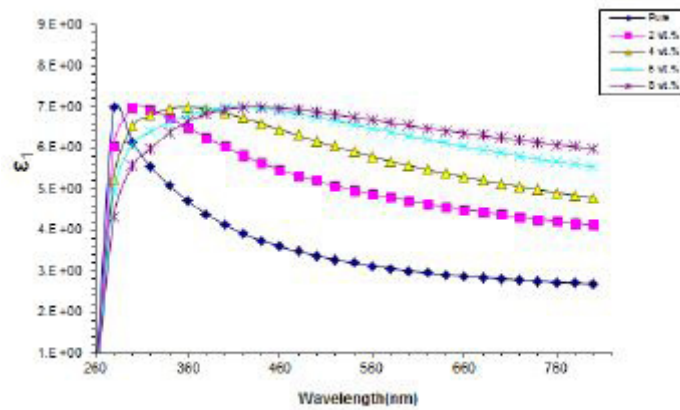


Fig. 11. Variation of real part of dielectric constant for (PS-In₂O₃/ ZnCoFe₂O₄) nanocomposites with wavelength .

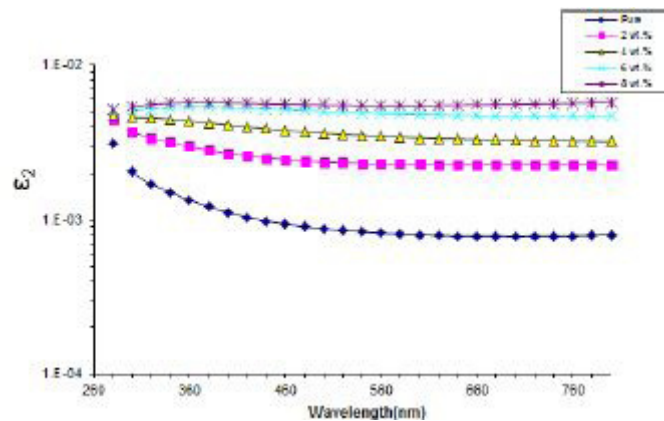


Fig. 12. Variation of imaginary part of dielectric constant for (PS-In₂O₃/ ZnCoFe₂O₄) nanocomposites with wavelength .

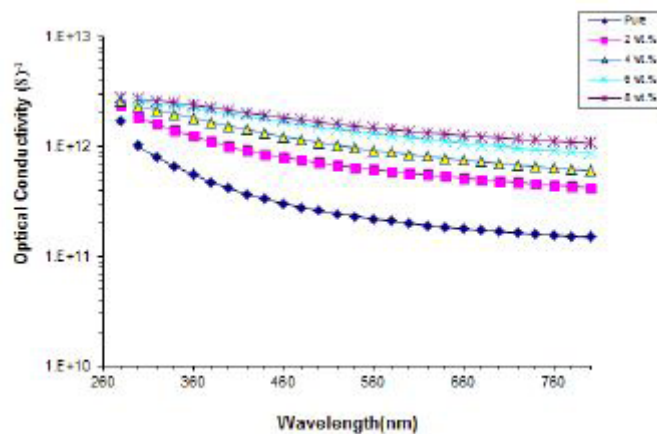


Fig. 13. Variation of optical conductivity for (PS- $\text{In}_2\text{O}_3/\text{ZnCoFe}_2\text{O}_4$) nanocomposites with wavelength

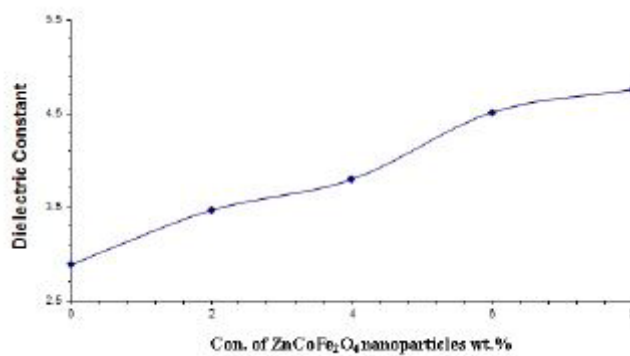


Fig. 14. The variation of dielectric constant with the concentration of filler at 100Hz

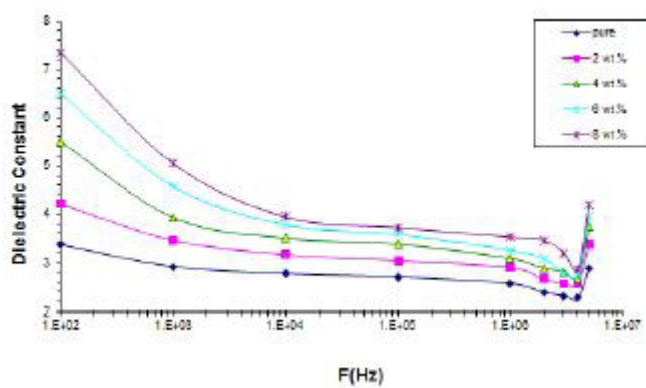


Fig. 15. The variation of dielectric constant with the frequency at room temperature.

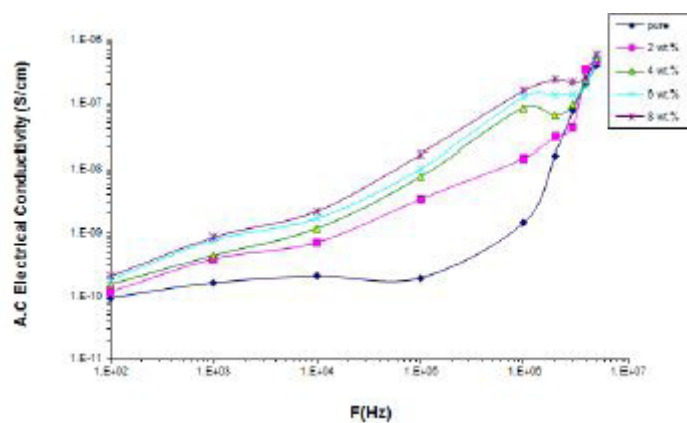


Fig. 16. The variation of electrical conductivity with the frequency at room temperature

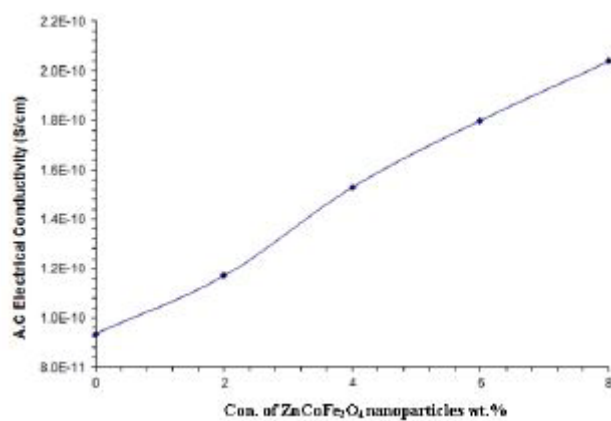


Fig. 17. The variation of A.C. electrical conductivity with the concentration of filler at 100Hz.

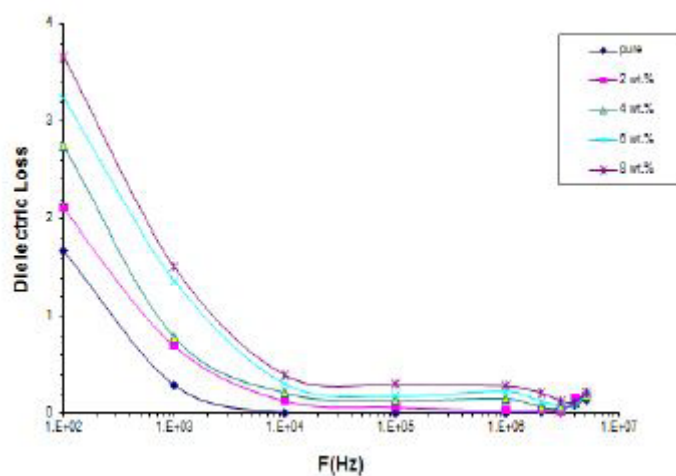


Fig. 18. The variation of dielectric loss with the frequency at room temperature.

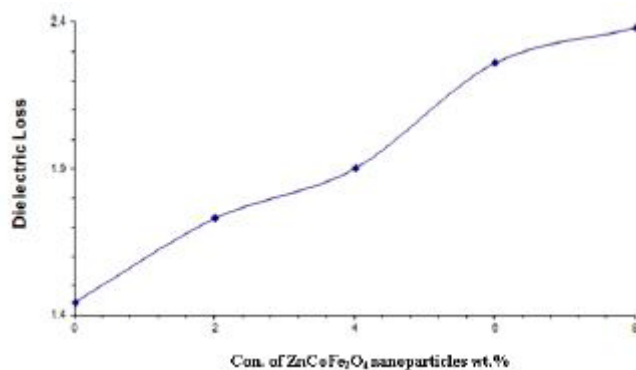


Fig. 19. The variation of dielectric loss with the concentration of filler at 100Hz.

References

- Imam, N.G. and Mohamed Bakr Mohamed, Environmentally friendly Zn_{0.75}Cd_{0.25}S/PVA heterosystemnanocomposite: UV-stimulated emission and absorption spectra, *Journal of Molecular Structure*, Vol.1105 (2016).
- Wasan Al-Taa'y, Mohammed Abdul Nabi, Rahimi M. Yusop, Emad Yousif, Bashar Mudhaffar Abdullah, Jumat Salimon, Nadia Salih, and Saifullrwan Zubairi, 2014, Effect of Nano ZnO on the Optical Properties of Poly(vinyl chloride) Films, *International Journal of Polymer Science*, ID. 697809, NO.6 (2014).
- Gon, M.; Tanaka, K.; Chujo, Y. Creative Synthesis of Organic–Inorganic Molecular Hybrid Materials. *Bull. Chem. Soc. Jpn.*, Vol. 90, 463–474. 2017.
- Okada, H.; Tanaka, K.; Chujo, Y., Preparation of Environmentally Resistant Conductive Silica-Based Polymer Hybrids Containing Tetrathiafulvalen-Tetracyanoquinodimethane Charge-Transfer Complexes. *Polym. J.*, Vol. 46, 800–805 (2014).
- K. Ueda, K. Tanaka, Y. Chujo, Optical, Electrical and Thermal Properties of Organic–Inorganic Hybrids with Conjugated Polymers Based on POSS Having Heterogeneous Substituents, *Polymers*, No.11, Vol.44 (2019).
- X.e Zhao, Y.Wu,a) Zhigang Fan, and Fei Li, Three-dimensional simulations of the complex dielectric properties of random composites by finite element method, *Journal of Applied Physics*, Vol.95, No.12, PP.(8110-8117) (2004).
- Qayssar M. Jebur, Ahmed Hashim, Majeed A. Habeeb, Structural, Electrical and Optical Properties for (Polyvinyl Alcohol–Polyethylene Oxide–Magnesium Oxide) Nanocomposites for Optoelectronics Applications, *Transactions on Electrical and Electronic Materials*, <https://doi.org/10.1007/s42341-019-00121-x>, (2019).
- Dezhi Qin, Guangrui Yang, Li Zhang, Xian Du, and Yabo Wang, Synthesis and Optical Characteristics, of PAM/HgSNanocomposites, *Journal of Bull. Korean Chem. Soc.*, Vol. 35, No. 4 (2014).
- Jassim, R.A.A. and Habeb, M.A., Effect of Cobalt Chloride (CoCl₂) on the Electrical and Optical Properties of (PVA-PVP-CoCl₂) Films“, *Advances in Physics Theories and Applications*, Vol.18, pp.47-53 (2013).
- Blythe, T. and Bloor, D. “*Electrical Properties of Polymers*”, 2nd ed., Cambridge University Press, UK, (2005)
- Zaky, A. A. and Hawley, R. “*Dielectric Solids, Dover*” pub., Inc. New York (1970).
- Abdullah1,O., Saber, D. R. and Hamasalih, L. O., “Complexion Formation in PVA/PEO/CuCl₂ Solid Polymer Electrolyte”, *Universal Journal of Materials Science*, Vol. 3, No. 1, PP.1-5 (2015).
- Elmarzugi,N., Adali, T., Bentaleb, A., Keleb, E. I., Mohamed, A. T. and Hamza, A. M., Spectroscopic Characterization of PEG- DNA Biocomplexes by FTIR, *Journal of Applied Pharmaceutical Science*, Vol.4, No. 8, PP. 6-10,(2014).
- Ahmed Hashim and Ali Jassim, Novel of (PVA-ST-PbO₂) Bio Nanocomposites: Preparation and Properties for Humidity Sensors and Radiation Shielding Applications, *Sensor Letters*, Vol. 15, No.12, (2017).
- Abbas, N.K., Habeeb, M.A. and Algidsawi, A.J.K. Preparation of Chloro penta amine cobalt(iii) chloride and study of its influence on the structural and some optical properties of polyvinyl acetate. *Int. J. Polymer Science*, <https://doi.org/10.1155/2015/926789> (2015).
- Hashim,A., Habeeb, M. A., Khalaf, A. and Hadi, A Fabrication of (PVA-PAA) Blend-Extracts of Plants Bio-Composites and Studying Their Structural, Electrical and Optical Properties for Humidity Sensors Applications, *Sensor Letters*, Vol.15, pp. 589–596 (2017).
- Falah Ali Jasim, Ahmed. Hashim, Angham. G. Hadi, Farhan Lafta, Saba R. Salman and Hind Ahmed, Preparation of (pomegranate peel-polystyrene) composites and study their optical properties, *Research Journal of Applied Sciences*, Vol.8, Issue. 9, PP. 439-441 (2013).
- Falah Ali Jasim, Farhan Lafta, Ahmed. Hashim, Majeed Ali, Angham. G. Hadi, Characterization of palm fronds-polystyrene composites, *Journal of Engineering and Applied Sciences*, Vol.8, No.5, PP. 140-142 (2013).
- Ahmed Hashim and Majeed Ali Habeeb, Structural and Optical Properties of (Biopolymer Blend-Metal Oxide) Bionanocomposites For Humidity Sensors, *Journal of Bionanoscience*, Vol.12, No.5 (2018).
- Ahmed Hashim, Majeed Ali Habeeb, and Aseel Hadi, Synthesis of Novel Polyvinyl Alcohol–Starch-Copper Oxide Nanocomposites for Humidity Sensors Applications with Different Temperatures, *Sensor Letters*, Vol.15, No.9, PP.758–761 (2017).
- Farhan Lafta Rashid, Aseel Hadi, Naheda Humood Al-Garah, Ahmed Hashim, Novel Phase

- Change Materials, MgO Nanoparticles, and Water Based Nanofluids for Thermal Energy Storage and Biomedical Applications, *International Journal of Pharmaceutical and Phytopharmacological Research*, Vol.8, Issue 1 (2018).
22. Ahmed Hashim and Majeed Ali Habeeb, Synthesis and Characterization of Polymer Blend- CoFe_2O_4 Nanoparticles as a Humidity Sensors For Different Temperatures, *Transactions on Electrical and Electronic Materials*, DOI: 10.1007/s42341-018-0081-1 (2019).
 23. Habeeb, M. A., Hashim, A. and Hadi, A., Fabrication of New Nanocomposites: CMC-PAA- PbO_2 Nanoparticles for Piezoelectric Sensors and Gamma Radiation Shielding Applications, *Sensor Letters*, Vol.15, No.9, PP. 785–790 (2017).
 24. Ahmed Hashim, Hayder Abduljalil, Hind Ahmed, Analysis of Optical, Electronic and Spectroscopic properties of (Biopolymer-SiC) Nanocomposites For Electronics Applications, *Egypt. J. Chem.*, DOI:10.21608/EJCHEM.2019.7154.1590 (2019).
 25. Ahmed Hashim, Zinah S. Hamad, Lower Cost and Higher UV-Absorption of Polyvinyl Alcohol/ Silica Nanocomposites For Potential Applications, *Egypt. J. Chem.*, DOI: 10.21608/EJCHEM.2019.7264.1593 (2019).
 26. Wadatkar, N.S., Waghuley, S.A., . Complex optical studies on conducting polyindole as-synthesized through chemical route. *Egypt. J. Basic Appl. Sci.* 2, 19 (2015).
 27. P. Guggilla, A. Chilvery, R. Powell. Reducing the bandgap energy via doping process in lead-free thin film nanocomposites. *Res. & Rev.: J. Mater. Sci.* 5, No. 1, 34 (2017).
 28. Ahmed Hashim, Majeed Ali Habeeb, Aseel Hadi, Qayssar M. Jebur, and Waled Hadi, Fabrication of Novel (PVA-PEG-CMC- Fe_3O_4) Magnetic Nanocomposites for Piezoelectric Applications, *Sensor Letters*, Vol.15, No.12 (2017).
 29. Hashim A and Hadi A. , Novel Pressure Sensors Made From Nanocomposites (Biodegradable Polymers–Metal Oxide Nanoparticles): Fabrication and Characterization. *Ukrainian Journal of Physics*, 63 (8), DOI:<https://doi.org/10.15407/ujpe63.8.754> (2018).
 30. Kadhim K J, Agool I R and Hashim A., Synthesis of (PVA-PEG-PVP- TiO_2) Nanocomposites for Antibacterial Application. *Materials Focus* 5 (5), DOI: <https://doi.org/10.1166/mat.2016.1371> (2016).
 31. Majeed Ali Habeeb, Ahmed Hashim, Abdul-Raheem K. AbidAli, The dielectric properties for (PMMA-LiF) composites , *European Journal of Scientific Research*, Vol. 61, No.3, pp.367-371, (2011).
 32. Ahmed Hashim and Zinah Sattar Hamad, Fabrication and Characterization of Polymer Blend Doped with Metal Carbide Nanoparticles for Humidity Sensors, *J. Nanostruct.*, Vol.9, No. 2, pp.340-348, (2019).
 33. Hind Ahmed, Ahmed Hashim and Hayder M. Abduljalil, Analysis of Structural, Electrical and Electronic Properties of (Polymer Nanocomposites / Silicon Carbide) for Antibacterial Application, *Egypt. J. Chem.*, Vol. 62, No. 4. pp.1167– 1176, DOI:10.21608/EJCHEM.2019.6241.1522 (2019).
 34. Ahmed Hashim, Hayder M. Abduljalil, Hind Ahmed, Fabrication and Characterization of (PVA- TiO_2) $_{1-x}$ / SiC_x Nanocomposites for Biomedical Applications, *Egypt. J. Chem.*, DOI: 10.21608/EJCHEM.2019.10712.1695 (2019).
 35. Hind Ahmed, Ahmed Hashim, Fabrication of PVA/ NiO/SiC Nanocomposites and Studying their Dielectric Properties For Antibacterial Applications, *Egypt. J. Chem.*, DOI: 10.21608/EJCHEM.2019.11109.1712 (2019).
 36. Qayssar M. Jebur, Ahmed Hashim, Majeed A. Habeeb, Fabrication, Structural and Optical properties for (Polyvinyl Alcohol–Polyethylene Oxide– Iron Oxide) Nanocomposites, *Egypt. J. Chem.*, DOI: 10.21608/EJCHEM.2019.10197.1669 (2019).
 37. Hashim A and Hadi A., synthesis and characterization of novel piezoelectric and energy storage nanocomposites: biodegradable materials–magnesium oxide nanoparticles. *Ukrainian Journal of Physics*, 62(12), doi: 10.15407/ujpe62.12.1050 (2017).
 38. Kadhim K J, Agool I R and Hashim A., Effect of Zirconium Oxide Nanoparticles on Dielectric Properties of (PVA-PEG-PVP) Blend for Medical Application. *Journal of Advanced Physics* 6 (2), DOI: <https://doi.org/10.1166/jap.2017.1313> (2017).

الخصائص التركيبية، والبصرية، العزلية للمترابكات (PS- In₂O₃/ ZnCoFe₂O₄) النانوية

نور حيدر، مجيد علي حبيب، احمد هاشم
جامعة بابل، كلية التربية للعلوم الصرفة، قسم الفيزياء، العراق

تم تحضير المترابكات (PS-In₂O₃/ ZnCoFe₂O₄) النانوية بطريقة صب المحلول. درست الخصائص التركيبية، البصرية، العزلية للمترابكات (PS-In₂O₃/ ZnCoFe₂O₄) النانوية لاستعمالها في التطبيقات البصرية والالكترونية المختلفة. تضمنت الخصائص التركيبية FTIR، والمجهر الضوئي، و SEM. بينت نتائج الخصائص البصرية للمترابكات (PS-In₂O₃/ ZnCoFe₂O₄) النانوية ان الامتصاصية، ومعامل الامتصاص، ومعامل الانكسار، ومعامل الخمود، وثوابت العزل والتوصيلية البصرية للمترابكات (PS-In₂O₃) النانوية تزداد مع زيادة تراكيز جسيمات ZnCoFe₂O₄ النانوية بينما النفاذية وفجوة الطاقة يقلان مع زيادة تراكيز جسيمات ZnCoFe₂O₄ النانوية. كما ان المترابكات (PS-In₂O₃/ ZnCoFe₂O₄) النانوية تمتلك امتصاصية عالية في المنطقة فوق البنفسجية. اوضحت نتائج الخصائص العزلية ان ثابت العزل، والفقدان العزلي والتوصيلة الكهربائية المتناوبة للمترابكات (PS-In₂O₃) النانوية تزداد مع زيادة تراكيز جسيمات ZnCoFe₂O₄ النانوية. ان ثابت العزل والفقدان العزلي يقلان بينما التوصيلية الكهربائية تزداد مع زيادة التردد.